Hyperfine Interact
DOI 10.1007/s10751-013-0768-y

Iron-bearing minerals in ashes emanated from Osorno volcano, in Chile

Alexandre Christófaro Silva · Mauricio Escudey · Juan Enrique Förster · Carmen Pizarro · José Domingos Ardisson · Uidemar Morais Barral · Márcio César Pereira · José Domingos Fabris

Abstract A sample of volcanic ashes emanated from the Osorno volcano, southern Chile, was characterized with X-ray fluorescence, X-ray diffraction and ^{57}Fe Mössbauer spectroscopy, in an attempt to identify the iron-bearing minerals of that geologically recent magmatic deposit. X-ray patterns indicated that the sample is mainly constituted of anorthite, Fe-diopside-type and Ca-magnetite. The crystallographic structures of these dominant iron minerals are proposed on basis of their chemical composition and corresponding Mössbauer data to support models refined by fitting powder X-ray diffraction data with the Rietveld algorithm.

Keywords Iron oxides · Magnetic minerals · Iron-rich spinel · Anorthite · Diopside

A. C. Silva · U. M. Barral · J. D. Fabris (✉)
Universidade Federal dos Vales do Jequitinhonha e Mucuri (UFVJM),
39100-000 Diamantina, Minas Gerais, Brazil
e-mail: jdfabris@ufmg.br

M. Escudey · J. E. Förster · C. Pizarro
Centro para el Desarrollo de la Nanociencia y Nanotecnología (CEDENNA),
Santiago 725475, Chile

M. Escudey · J. E. Förster · C. Pizarro
Facultad de Química y Biología, Universidad de Santiago de Chile, USACH,
Santiago 725475, Chile

J. D. Ardisson
Centro de Desenvolvimento da Tecnologia Nuclear,
31270-901 Belo Horizonte, Minas Gerais, Brazil

M. C. Pereira
Instituto de Ciência, Engenharia e Tecnologia, Universidade Federal dos Vales do Jequitinhonha e Mucuri, 39803-371 Teófilo Otoni, Minas Gerais, Brazil

Published online: 09 February 2013

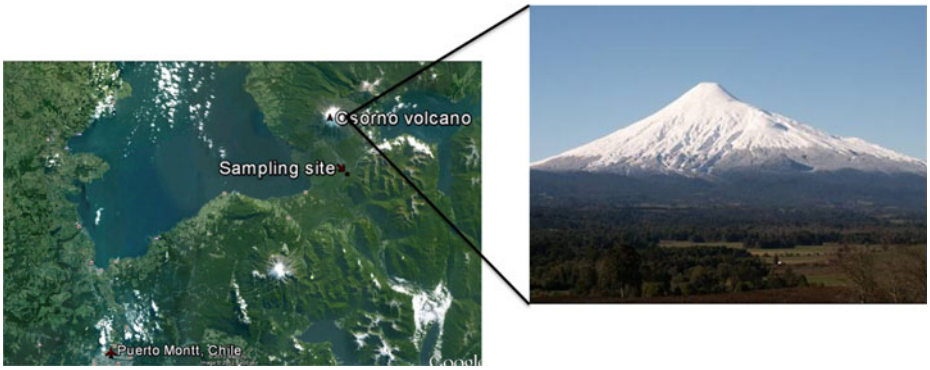

Fig. 1 Osorno volcano in the Los Lagos Region, Puerto Montt, Southern Chile

1 Introduction

Soils derived from volcanic materials are abundant and widespread all over the southern Chile. They actually account for around 70 % of the Chilean land areas covered with agriculture crops. Blasted ashes spread out around a large perimeter and lava flows surrounding the volcanic source lead to consolidate magmatic rocks, which markedly influence the lithogenic parent materials on which such soils develop. Resulting pedons are mainly characterized by having high clay and iron (oxyhydr)oxides contents. Most of those soils are magnetic for containing important amounts of magnetite (ideal formula, Fe_3O_4) or maghemite (γFe_2O_3) [1–6].

The problem concerning the nature of precursor minerals and their chemical and mineralogical changes during pedogenesis, to render the currently found magnetic iron oxides, still remains to be better elucidated. The purpose of this work was to look somewhat closer in an attempt to identify in more detail the iron-bearing chemical species occurring in ashes forming the parent material of volcanic soils, which could be the elemental source or direct precursor of iron oxides found in the corresponding pedon.

2 Materials and methods

A sample of volcanic ashes was collected at a depth between 200 cm and 220 cm in a dug pit (geographical coordinates of the sampling site, 41° 11′ 37.47″ S 72° 28′ 31.52″ W; altitude, 104 m) on the flow way of geologically recent lavas and ashes, surrounding the volcanic source Osorno, in the Los Lagos Region, Puerto Montt, southern Chile (Fig. 1). In the laboratory, the sample was dried in air and ground in an agate mortar. This sample of volcanic ashes was characterized with powder X-ray diffraction (XRD) measurements, using a Shimadzu XRD 6000 diffractometer equipped with a Cu tube and a graphite monochromator. The scans were performed between 10 and 80° (2θ) with a scanning speed of 1°/min. Silicon was used as an external standard. The Rietveld structural refinement was performed with FULLPROF 2012 program (code available

Table 1 Crystallographic phase, lattice parameter and agreement factor values as obtained from the structural refinement with Rietveld algorithm for this volcanic ash sample

Phase	Lattice parameter/Å	Bragg R-factor	R_f-Factor	R_p	R_{wp}
Anorthite	a = 8.1681(3) b = 12.8663(4) c = 7.0980(2)	4.53	4.46	4.18	5.66
Fe-diopside-type	a = 9.7392(6) b = 8.9134(4) c = 5.2809(3)	3.69	3.83		
Ca-magnetite	a = 8.4205(5)	2.39	1.54		

at http://www.ill.eu/sites/fullprof/php/downloads.html). X-ray fluorescence (XRF) spectrometry measurement was performed on a S4 explorer X-ray spectrometer (Bruker-AXS, Germany).

Mössbauer spectra were collected in constant acceleration transmission mode with a ~30 mCi ^{57}Co/Rh source. The spectra were obtained at 298 K and 80 K using a liquid-N_2 bath cryostat. Data were stored in a 512-channel MCS memory unit. The collected experimental data were fitted with Lorentzian-shape resonance lines through a least-squares procedure of the software NORMOS™-90 (software package developed by R. A. Brand, at Laboratorium für Angewandte Physik, Universität Duisburg, D-47048, Duisburg-Germany); isomer shifts are quoted relative to α-Fe.

3 Results and discussion

XRF analysis revealed that this sample of volcanic ashes is basically constituted of 60 mass% Si; 24.5 mass% Al; 6.9 mass% Fe; 6.8 mass% Ca; 0.7 mass% Ti and 0.7 mass% K. Its mineralogical composition was first inferred from a phase search based on data of the powder XRD pattern. Further Rietveld refinement of these XRD data with pseudo-Voigt peak fitting gave the structural parameters of each crystalline phase and the refinement reliability factors summarized in Table 1. Figure 2 shows patterns from the corresponding Rietveld refinement. This analysis reveals that the volcanic ashes sample is constituted of 79 mass% anorthite (ideal formula, $CaAl_2Si_2O_8$), 17 mass% Fe-diopside-type ($CaFeSi_2O_6$) and 4 mass% Ca-magnetite ($Fe_{3-x}Ca_xO_4$). Although the XRD data were fitted assuming three dominant phases, contributions of other minor crystalline species cannot be excluded.

Although XRD data provide information about the crystallographic structure, the Fe distribution per mineral structure may not be directly determined this way. It was therefore used ^{57}Fe Mössbauer spectroscopy data to define the Fe sites in each structure so found from the XRD analysis. Mössbauer spectra for the volcanic ashes sample collected at 298 and 80 K are shown in Fig. 3. The 298 K Mössbauer spectrum was fitted with two magnetic components and three paramagnetic components. The sextet-components are assignable to a tetrahedral Fe^{3+} site and to a mixture of octahedral $Fe^{2+/3+}$ ions, which is due to the fast electron hopping, in the magnetite

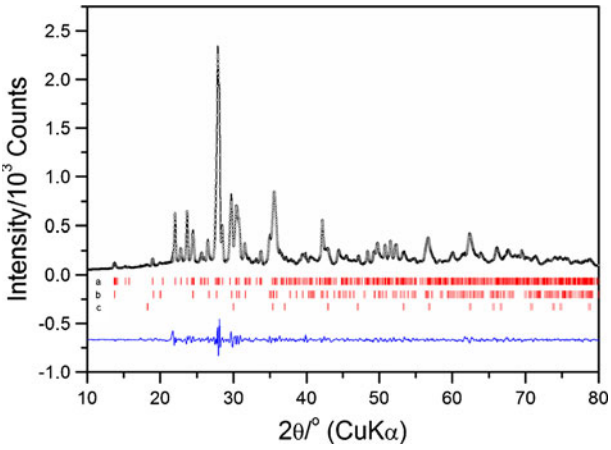

Fig. 2 Rietveld refinement on the powder XRD pattern of the volcanic ashes sample. a = Anorthite, b = Fe-diopside-type structure and c = Ca-magnetite

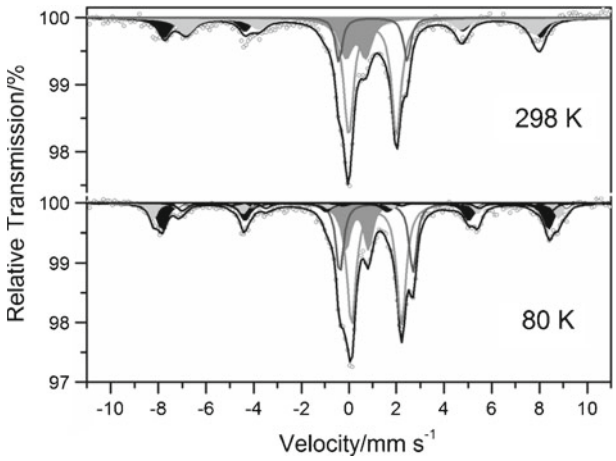

Fig. 3 298 and 80 K Mössbauer spectra for the volcanic ashes sample

structure (Table 2). Doublets are due to Fe^{2+} on octahedral (M1) and dodecahedral (M2) positions of the Fe-diopside-type structure (Table 2). The Fe^{3+} doublet could be appeared as due to the oxidation of Fe^{2+} oxidation on the M1 site in the Fe-diopside-type structure.

80 K-Mössbauer spectrum of volcanic ashes sample (Fig. 3) was fitted with three doublets corresponding to Fe in the Fe-diopside-type structure and three sextets due to iron in the magnetite. It is known that pure magnetite undergoes Verwey transition around 120 K, which is also related to the charge ordering of Fe^{2+} and Fe^{3+} ions in octahedral sites, but the mechanism is still not sufficiently known. Some reports have proposed that the Mössbauer spectrum for pure magnetite below Verwey transition should be fitted with five spectral components: one related to Fe^{3+} ions on the tetrahedral sites and four corresponding to Fe^{2+} or Fe^{3+} ions on two nonequivalent octahedral sites [7, 8]. The Mössbauer spectrum for the volcanic ashes collected with the sample at 80 K was accordingly fitted with a magnetic

Table 2 Hyperfine parameters of the fitted Mössbauer spectra recorded at 298 and 80 K

Temperature/K	δ/mm s^{-1}	ε, Δ/mm s^{-1}	B_{hf}/T	RA/%	^{57}Fe site
298	0.29(1)	−0.05	49.0(2)	16(1)	$^{IV}Fe^{3+}$
	0.59(2)	0.05(2)	45.5(2)	18(2)	$^{VI}Fe^{2.5+}$
	0.41(2)	0.83(3)	–	16(1)	$^{VI}Fe^{3+}$
	1.11(3)	2.01(3)	–	39(2)	$^{VI}Fe^{2+}$
	1.12(1)	2.86(2)	–	11(1)	$^{VIII}Fe^{2+}$
80	0.39(2)	−0.07	50.3(2)	18(1)	$^{IV}Fe^{3+}$
	0.50(2)	−0.18	52.4(1)	7(1)	$^{VI}Fe^{3+}$
	0.92(1)	0.32(2)	50.7(2)	3(1)	$^{VI}Fe^{2+}$
	0.98(2)	−0.25	48.0(1)	5(1)	$^{VI}Fe^{2+}$
	1.09(1)	0.90(2)	39.5[a]	2(1)	$^{VI}Fe^{2+}$
	0.46(3)	0.95(3)	–	13(1)	$^{VI}Fe^{3+}$
	1.27(2)	2.10(5)	–	36(2)	$^{VI}Fe^{2+}$
	1.27(3)	3.06(7)	–	17(1)	$^{VIII}Fe^{2+}$

δ = isomer shift relative to α-Fe; ε = quadrupole shift; Δ = quadrupole splitting; B_{hf} = hyperfine field and RA = relative subspectral area

[a]Parameter kept fixed during fitting convergence

Fe^{3+} component at tetrahedral coordination and four magnetic Fe components in octahedral coordination: one sextet for Fe^{3+} and three sextets for Fe^{2+} (Table 1), which correspond to the different Fe^{2+} environment in the magnetite structure. Although the proposal model involves only the occurrence of magnetite as the magnetically ordered specie, eventual contributions of maghemite and/or hematite cannot be completely discarded.

The relative area ratio (RA; Table 2) between octahedral (B) and tetrahedral sites (A), $\frac{(RA)_B}{[RA]_A} = 1.1$, at 298 K, which is far below the value expected for stoichiometric magnetite, $\frac{(RA)_B}{[RA]_A} = 1.88$. The found occupancy ratio for this magnetite is determined by taking into account that the recoilless fraction for octahedral (B) sites is 6 % lower than that for tetrahedral [A] sites [9], or $R = \frac{(Fe^{\frac{3+}{2+}})_B}{[Fe^{3+}]_A} = \frac{\frac{(RA)_B}{0.94}}{[RA]_A} = \frac{\frac{18}{0.94}}{16} = 1.2$. Actually, there are two main factors that lead to $R = \frac{(Fe^{\frac{3+}{2+}})_B}{[Fe^{3+}]_A} < 2$ in magnetite: (i) an oxidation mechanism involving $Fe^{2+} \Rightarrow Fe^{3+}$ and (ii) isomorphic replacement of Fe by other cations. In the first case, for each three Fe^{2+} that oxidizes, two Fe^{3+} are formed and one cationic vacancy is created, in order to maintain the charge balance in the chemical structure. The high spin Fe^{3+} ionic radium on octahedral coordination is $r = 65$ pm; for Fe^{2+}, $r = 78$ pm. Thus, the oxidation of Fe^{2+} to Fe^{3+} would lead to a decreasing of the cubic unit cell dimension of magnetite. Our Rietveld results evidence that the lattice parameter of magnetite (Table 1) in this sample is higher than that expected for pure and stoichiometric magnetite, suggesting an isomorphic substitution of iron by other cations with higher ionic radium than those reported for Fe^{3+} or Fe^{2+} ions. Based on the fluorescence analysis, we suggest that Fe^{2+} ions in the magnetite structure are partially replaced by Ca^{2+} (ionic radium, $r = 100$ pm) ions, which causes significant expansion of the magnetite cubic structure. Thus, the isomorphic replacement of Fe^{2+} by Ca^{2+} should increase the unit cell of magnetite, as it was observed from Rietveld analysis.

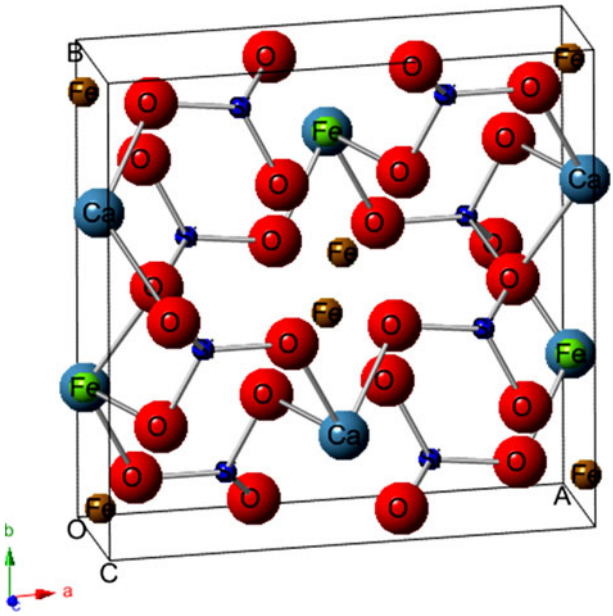

Fig. 4 Crystallographic structure of this Fe-diopside-type

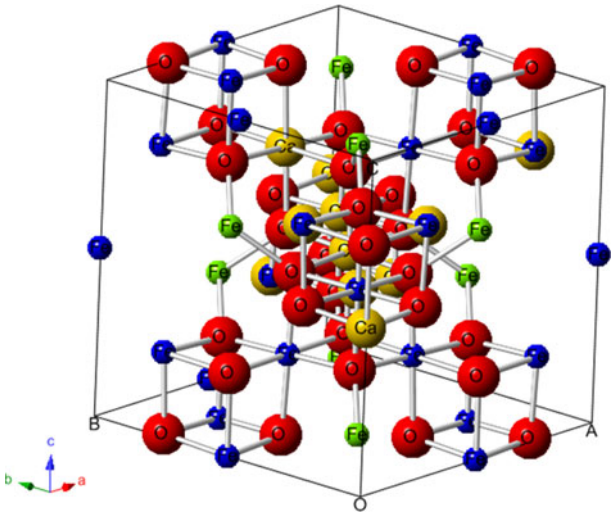

Fig. 5 Crystallographic structure of this Ca-magnetite

The Fe-diopside-type structure is monoclinic, space group $C2/c$. The Ca^{2+} cations are located in eightfold (M2 sites) oxygen-coordination sites. The Fe^{2+} cations are located in both M2 sites and in sixfold (M1 sites) oxygen-coordination sites, as confirmed by Mössbauer spectroscopy.

The crystallographic structures, as deduced from the Rietveld refinement of the powder X-ray data, for the Fe-diopside-type and Ca-magnetite of this Ca-rich sample from volcanic ashes are represented in Figs. 4 and 5, respectively.

4 Conclusions

The mineralogy of this sample of volcanic ashes sample, which is relatively rich in calcium, is dominantly constituted of anorthite, Fe-diopside-type and Ca-magnetite. Mössbauer parameters are consistent with iron in octahedral (B) and tetrahedral [A] coordination sites of the magnetite (with a ratio $R = \frac{(Fe^{\frac{3+}{2+}})_B}{[Fe^{3+}]_A} = 1.2$) and in the octahedral and at dodecahedral sites of the Fe-diopside-type structure. The crystallographic structure for these Fe-diopside-type and Ca-doped magnetite are proposed basing on fitting powder X-ray diffraction data by using the Rietveld algorithm, and chemical composition deduced from X-ray fluorescence data. Progressive weathering processes acting on this magmatic magnetite should respond for structural alterations to ultimately form the magnetic iron oxides found in Chilean soils. Further Mössbauer measurements, as with applied magnetic field, would be interesting, in order to definitively confirm this interpretation concerning the iron distribution in minerals of this sample.

Acknowledgements Work financially supported by DICYT-USACH 0221242PA, CEDENNA FB-0807 (Chile), CNPq (Brazil; grants #480295/2009-3; #302479/2010-4 and PROSUL #490096/2010-7) and FAPEMIG (Brazil; including #PPM 00419-10 and #APQ-04333-10). CAPES (Brazil) grants the Visiting Professor PVNS fellowship to JDF at UFVJM

References

1. Pizarro, C., Furet, N.R., Venegas, R., Fabris, J.D., Escudey, M.: Some cautions on the interpretation of Mossbauer spectra in mineralogical studies of volcanic soils. Bol. Soc. Chil. Quim. **45**, 243–250 (2000)
2. Pizarro, C., Escudey, M., Fabris, J.D., Almeida, A.B.: Iron-rich spinel phases from the sand fraction of three Chilean soils developing on volcanic materials. Comm. Soil Sci. Plan. **32**, 2741–2754 (2001)
3. Pizarro, C., Escudey, M., Fabris, J.D.: Influence of organic matter on the iron oxide mineralogy of volcanic soils. Hyperfine Interact. **148**, 53–59 (2003)
4. Pizarro, C., Escudey, M., Moyá, S.A., Fabris, J.D.: Iron oxides from volcanic soils as potential catalysts in the water gas shift reaction. In: Garcia, M., Marco, J.F., Plazaola, F. (eds.) Industrial Applications of the Mössbauer Effect—International Symposium on the Industrial Applications of the Mössbauer Effect, 765 ed., American Institute of Physics - AIP Conference Proceedings, New York, vol. 765, p. 56–59 (2005)
5. Pizarro, C., Fabris, J.D., Stucki, J.W., Garg, V.K., Morales, C., Aravena, S., Gautier, J.L., Galindo, G.: Distribution of Fe-bearing compounds in an Ultisol as determined with selective chemical dissolution and Mössbauer spectroscopy. Hyperfine Interact. **175**, 95–101 (2007)
6. Aravena, S., Pizarro, C., Rubio, M.A., Cavalcante, L.C.D., Garg, V.K., Pereira, M.C., Fabris, J.D.: Magnetic minerals from volcanic Ultisols as heterogeneous Fenton catalysts. Hyperfine Interact. **195**, 35–41 (2010)
7. Hargrove, R.S., Kündig, W.: Mössbauer measurements of magnetite below the Verwey transition. Solid State Commun. **8**, 303–308 (1970)
8. Berry, F.J., Skinner, S., Thomas, M.F.: ^{57}Fe Mössbauer spectroscopic examination of a single crystal of Fe_3O_4. J. Phys. Condens. Matter **10**, 215–220 (1998)
9. Sawatzky, G.A., van der Woude, F., Morrish, A.H.: Recoilless-fraction ratios for Fe^{57} in octahedral and tetrahedral sites of a Spinel and a Garnet. Phys. Rev. **183**, 383–386 (1969)